


Original Research

Neuroprotection against Aluminum Chloride-Induced Hippocampus Damage in Albino Wistar Rats by *Leucophyllum frutescens* (Berl.) I.M. Johnst. Leaf Extracts: A Detailed Insight into Phytochemical Analysis and Antioxidant and Enzyme Inhibition Assays

Imtiaz Ahmad^{1,2,3}, Saeed Ahmad¹, Esra Küpeli Akkol^{4,*} , Huma Rao¹,
Muhammad Nadeem Shahzad¹, Mehwish Nawaz⁵, Bilal Ahmad Ghalloo¹,
Wayne Thomas Shier³, Eduardo Sobarzo-Sánchez^{6,7,*}

¹Department of Pharmaceutical Chemistry, Faculty of Pharmacy, The Islamia University of Bahawalpur, 63100 Punjab, Pakistan

²Primary and Secondary Health Care Department, Government of Punjab, 63100 Punjab, Pakistan

³Department of Medicinal Chemistry, College of Pharmacy, University of Minnesota, Minneapolis, MN 55455, USA

⁴Department of Pharmacognosy, Faculty of Pharmacy, Gazi University, 06330 Ankara, Turkey

⁵Department of Pharmaceutics, Faculty of Pharmacy, The Islamia University of Bahawalpur, 63100 Punjab, Pakistan

⁶Instituto de Investigación y Postgrado, Facultad de Ciencias de la Salud, Universidad Central de Chile, 8330507 Santiago, Chile

⁷Department of Organic Chemistry, Faculty of Pharmacy, University of Santiago de Compostela, 15782 Santiago de Compostela, Spain

*Correspondence: esrak@gazi.edu.tr (Esra Küpeli Akkol); eduardo.sobarzo@ucentral.cl (Eduardo Sobarzo-Sánchez)

Academic Editor: Luigi De Masi

Submitted: 19 April 2023 Revised: 3 July 2023 Accepted: 17 July 2023 Published: 28 August 2023

Abstract

Background: A previously unstudied medicinal plant, *Leucophyllum frutescens* (Berland.) I.M. Johnst. (Scrophulariaceae) was investigated to evaluate its potential in preventing and treating neurodegenerative diseases, including Alzheimer's disease. **Methods:** Methanolic leaf extract (MELE) and its fractions (HELE, CHLE, and BULE) were evaluated for their polyphenolic content and antioxidant activity by five different methods, including *in vitro* enzyme inhibition assays, which are clinically linked to neurodegenerative diseases. The potentially active *n*-butanol fraction (BULE) was further evaluated for its neuroprotective effects using an albino rat animal model and phytoconstituents profiling using Liquid chromatography with tandem mass spectrometry (LC-MS/MS), and *in silico* molecular docking by Maestro® Schrödinger. **Results:** The *n*-butanol fraction (BULE) in the hydroalcoholic leaf extract exhibited the highest total phenolic content (230.435 ± 1.575 mg gallic acid equivalent $\text{gm}^{-1} \pm \text{SD}$). The chloroform leaf extract exhibited the highest total flavonoid content (293.343 ± 3.756 mg quercetin equivalent $\text{gm}^{-1} \pm \text{SD}$) as well as the highest antioxidant content, which was equivalent to Trolox, with five assay methods. Similarly, the chloroform and *n*-butanol fractions from the hydroalcoholic leaf extract significantly inhibited human acetylcholinesterase and butyrylcholinesterase with their IC_{50} values of 12.14 ± 0.85 and 129.73 ± 1.14 $\mu\text{g}\cdot\text{mL}^{-1}$, respectively. The *in vivo* study revealed that BULE exhibited a significant neuroprotective effect at doses of 200 and 400 mg/kg/day in an aluminum chloride-induced neurodegenerative albino rat model. The LC-MS/MS analysis of BULE tentatively confirmed the presence of biologically active secondary metabolites, such as theobromine, propyl gallate, quercetin-3-O-glucoside, myricetin-3-acetyl-rhamnoside, isoquercitrin-6'-O-malonate, diosmetin-7-O-glucuronide-3'-O-pentose, pinoresinol diglucoside, asarinin, eridictoyl, epigallocatechin, methyl gallate derivative, and eudesmin. The results from the computational molecular docking of the identified secondary metabolites revealed that diosmetin-7-O-glucuronide-3'-O-pentose had the highest binding affinity to human butyrylcholinesterase, while isoquercetin-6'-O-malonate had the highest to human acetylcholinesterase, and pinoresinol diglucoside to human salivary alpha-amylase. **Conclusions:** The present study concluded a need for further exploration into this medicinal plant, including the isolation of the bioactive compounds responsible for its neuroprotective effects.

Keywords: antioxidant activity; enzyme inhibition assay; liquid chromatography-mass spectrometry; *Leucophyllum frutescens*; Scrophulariaceae; polyphenolic content

1. Introduction

Dementia is a chronic and progressive neurodegenerative disease that impacts more than 55 million older people worldwide [1]. The most frequent form of dementia in older people is Alzheimer's disease (AD), with age, genetics, and traumatic brain damage all being contributory elements to its onset, which ultimately, leads to mor-

talidity through the loss of cognitive function [2]. In the US, AD accounts for 60–70% of the decline in cognitive function in the elderly and is the seventh largest cause of death [3]. In Pakistan, the WHO reported in 2020 that dementia and AD were responsible for 1.3% of all mortality worldwide [4]. The buildup of various-sized hyperphosphorylated beta-amyloid and tau proteins in neural fibers



is a hallmark of the histopathology of Alzheimer's disease [5]. Unfortunately, the development of safe and effective disease-modifying drugs to treat the cognitive problems experienced by dementia patients has started to lag. However, a recently approved monoclonal antibody drug, lecanemab-irmb (Leqembi®), may delay cognitive decline, and thus, represent a change in the history of AD therapy. Over the past two decades, tacrine, a centrally acting acetylcholinesterase inhibitor with indirect cholinergic agonist action, was withdrawn from the market due to hepatotoxicity, thereby leaving cholinesterase inhibitors (e.g., donepezil, galantamine, and rivastigmine) and N-methyl-D-aspartate (NMDA) antagonists (e.g., memantine HCl) as the only medications approved for the treatment of AD [5]. Studies on phytochemicals that inhibited acetylcholine esterase and butyrylcholine esterase showed that they produced higher levels of acetylcholine in the synaptic cleft, which promoted neurotransmission and resulted in increased cognitive responses [6]. A study where 150 lignans were used as inhibitors of various target enzymes, known to be involved in several oxidative pathways, concluded that 139 of the lignans inhibited two or more of the studied enzymes, including JNK-3, PTIB, NOX1, etc. [7]. Polyphenolic compounds have previously been used to treat various neurological disorders, such as Parkinson's and Alzheimer's disease. Lignans, which are found in a variety of plant sources, have been studied for their neuroprotective effects in H₂O₂-induced oxidatively stressed neuroblastoma SH-SY5Y cell lines [8]. When the cytotoxic effects of sesamin, a lignan from sesame oil, and its derivative 3-bis-(3-methoxybenzyl)butane-1,4-diol (BBD) were examined in association with beta-amyloid proteins in PC12 cells, it was found that the derivative significantly downregulated beta-amyloid-induced JNK, ERK, MAPK, P38 pathways, and Bax expression in the cells. Asiasari radix extracts containing the furanofuran lignan diaspartemin, which was previously identified from the bark of *L. frutescens*, were demonstrated to ameliorate the cognitive behavior associated with sporadic Alzheimer's disease and boost insulin receptor sensitivity in rats and mice [9]. Potential neuroprotective drugs, which might be utilized to stop the progression of this group of disorders, include enzyme inhibitors that mediate the pathology of Alzheimer's and other neurodegenerative diseases. Alkaloids, flavonoids, and lignans are only a few of the secondary metabolites that are abundant in *L. frutescens* and might be used as potential inhibitors of the enzymes that hydrolyze acetylcholine [9]. The lignans of *L. frutescens* include members of the furanofuran subclass of lignans (Fig. 1).

Numerous studies [10] have demonstrated that people with diabetes mellitus have an increased risk of developing AD, although the underlying biological mechanism(s) linking the two diseases is unclear. Diabetes mellitus is characterized by high blood glucose levels (hyperglycemia), characterized by the destruction of pancreatic β -cells, and re-

sults in low levels of insulin secretion (Type 1 DM), reduced responsiveness of target tissues to insulin (Type 2 diabetes mellitus (DM)), or both. Elevated blood glucose levels are associated with long-term damage to various tissue types, notably nerves. The exact mechanism(s) through which hyperglycemia causes tissue damage is not well understood, although is widely thought to include the high-level production of reactive oxygen species [11]. The usual approach for preventing hyperglycemia-induced tissue damage is to prevent hyperglycemia by using one or more of a variety of different treatment modalities to control postprandial glucose levels. Among the possible treatment modalities is the inhibition of enzymes that convert polysaccharides to glucose, such as alpha-amylase, which forms disaccharides from starch, and alpha-glucosidase, which makes glucose readily available for absorption and maintains blood glucose levels [12].

There are various strategies being considered for directly treating or mitigating Alzheimer's disease. Currently, a common strategy is the inhibition of acetylcholinesterase (AChE) and butyrylcholinesterase [5]. Native Americans have used the leaf decoction of *Leucophyllum frutescens* (Berland.) I.M. Johnston, known as Cenizo, for its mild sedative effects in addition to treating lung congestion, bronchitis, and chills associated with the common cold [13]. The aim of this study was to evaluate the potential of this plant against AD. Thus, a hydroalcoholic leaf extract (MELE) and its three different solvent fractions (HELE, CHLE, and BULE) were obtained and evaluated as potential sources of neuroprotective agents by examining their polyphenolic content, antioxidant potential, ability to inhibit enzymes clinically linked to neurodegeneration, and neuroprotection in an animal model.

2. Materials and Methods

2.1 Study Approval and Plant Specimen Identification

This study was approved by the Advanced Studies and Research Board of the Islamia University of Bahawalpur, via letter No. 673/AS&RB, dated December 16, 2019. The plant was purchased from a local nursery for authentication by a taxonomist at the Herbarium Department of Botany, Faculty of Life Sciences, The Islamia University of Bahawalpur (Ref no. 60/botany; dated September 25, 2018).

2.2 Chemicals

Ammonium acetate, ferric chloride, methanol, absolute ethanol, *n*-hexane, chloroform, *n*-butanol, dimethyl sulfoxide, deionized water, and hydrogen peroxide were purchased from Merck KGaA (Darmstadt, Germany). All other chemicals, including acetylcholinesterase from human erythrocytes (C0663), butyrylcholinesterase from equine serum (C0157), alpha-amylase from human saliva (A1031; type XIII-A), 2,2-diphenyl-1-picrylhydrazyl (DPPH), 2,2-azino-bis (3-ethylbenzothiazoline), 6-sulfonic

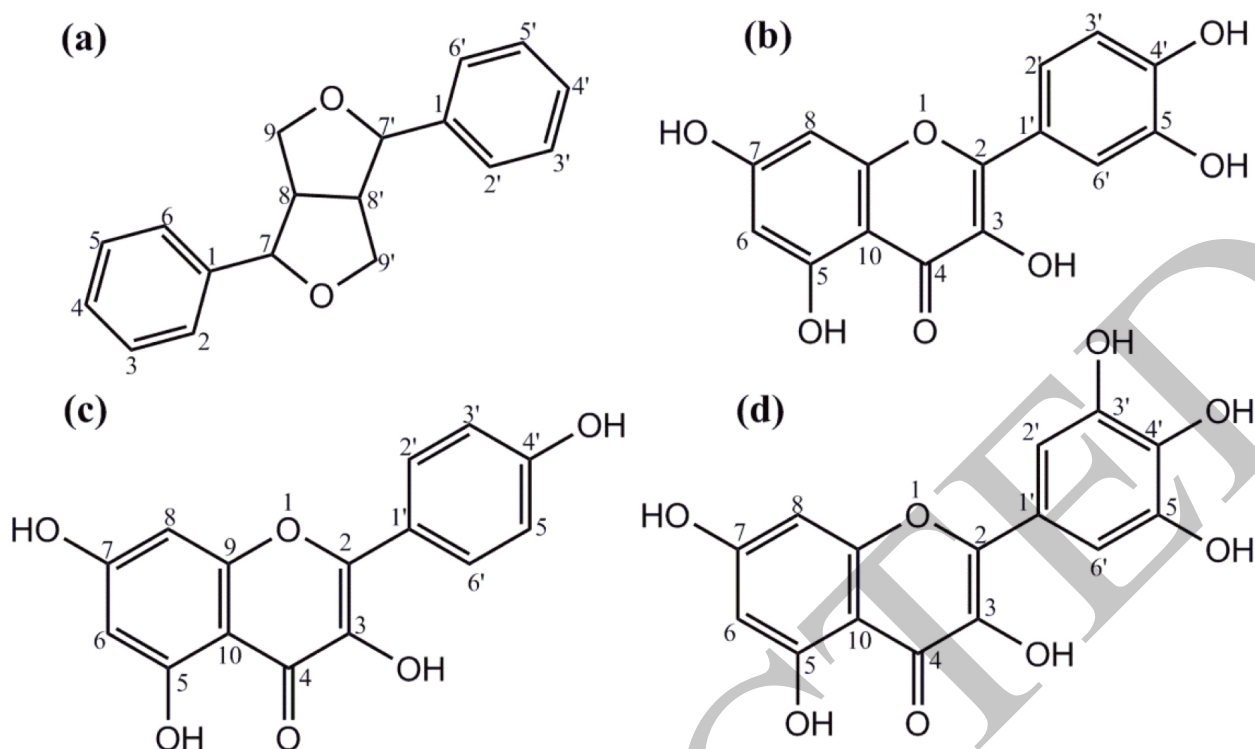


Fig. 1. Structures of phenolics and flavonoids. (a) The furanofuran lignan backbone and general structure are found in many plant-derived phenolics. Structures of some flavonoids found in *L. frutescens* leaf extracts: (b) quercetin, (c) kaempferol, and (d) myricetin.

acid, 2,4,6-tris (2-pyridyl)-s-triazine (TPTZ), and neocuproine were purchased from Sigma-Aldrich, St. Louis, MO, USA.

2.3 Solvent Extraction and Fractionation of *L. frutescens* Leaf

The 200 intact *L. frutescens* were purchased from a nearby nursery in Bahawalpur, Pakistan (29°23'42.0''N 71°39'46.8''E), and afterwards cultivated on a private piece of land. The leaves were collected, shade-dried, and pulverized. The pulverized leaf material weighed 5 kg and was macerated in 30 L of 80% aqueous methanol for 15 days, with occasional shaking. The menstruum was collected, filtered, and then, evaporated at 40 °C using a rotary evaporator. The retained part was discarded. A sample of the dried leaf residue was dissolved in methanol at 200 mg/mL to provide the methanol leaf extract (MELE). Dried leaf extract (150 g) was suspended in 500 mL of water and extracted in 5 L of *n*-hexane. The *n*-hexane phase was evaporated using a rotary evaporator to give the *n*-hexane fraction of hydroalcoholic leaf extract (HELE). The aqueous phase was extracted using 5 L of chloroform, and the resulting chloroform phase was evaporated using a rotary evaporator to provide the chloroform fraction of the hydroalcoholic leaf extract (CHLE). The aqueous phase was extracted using 5 L of *n*-butanol and the resulting *n*-butanol phase was evaporated using a rotary evaporator to produce the *n*-butanol fraction of the hydroalcoholic leaf extract (BULE).

2.4 Phytochemical Screening and Polyphenolic Contents

The qualitative analysis of secondary metabolites was performed according to the methods described in Trease and Evan's Pharmacognosy [14]. Total phenolic content was determined colorimetrically using Folin and Ciocalteu's phenol reagent [15]. The total phenolic content values were calculated using the straight-line equation, $Y = 0.0105x + 0.0702$, in which Y is the absorbance of the sample and x is the amount of total phenolic content in $\mu\text{g}\cdot\text{mL}^{-1}$, which was used to calculate the mg gallic acid equivalent per gram of dry extract ($\text{mg GA}\cdot\text{Eq}\cdot\text{gm}^{-1}$ DE) using the formula $C = xV/M$, where C is the mg gallic acid equivalent per gram of dry extract, V is the used sample volume in mL, and M is the weight of the sample used in grams. Total flavonoid content was determined using the aluminum chloride colorimetric assay [16] and was also calculated using the straight-line equation $Y = 0.0014x + 0.0293$, in which Y is the absorbance of the sample and x is the amount of total flavonoid content in $\mu\text{g}\cdot\text{mL}^{-1}$, which was used to calculate quercetin equivalent per gram of the dry weight of extract ($\text{mg Que}\cdot\text{Eq}\cdot\text{gm}^{-1}$ of DE) using the formula $C = xV/M$, where C is the mg quercetin equivalent per gram of dry extract, V is the used sample volume in mL, and M is the weight of the sample in grams.

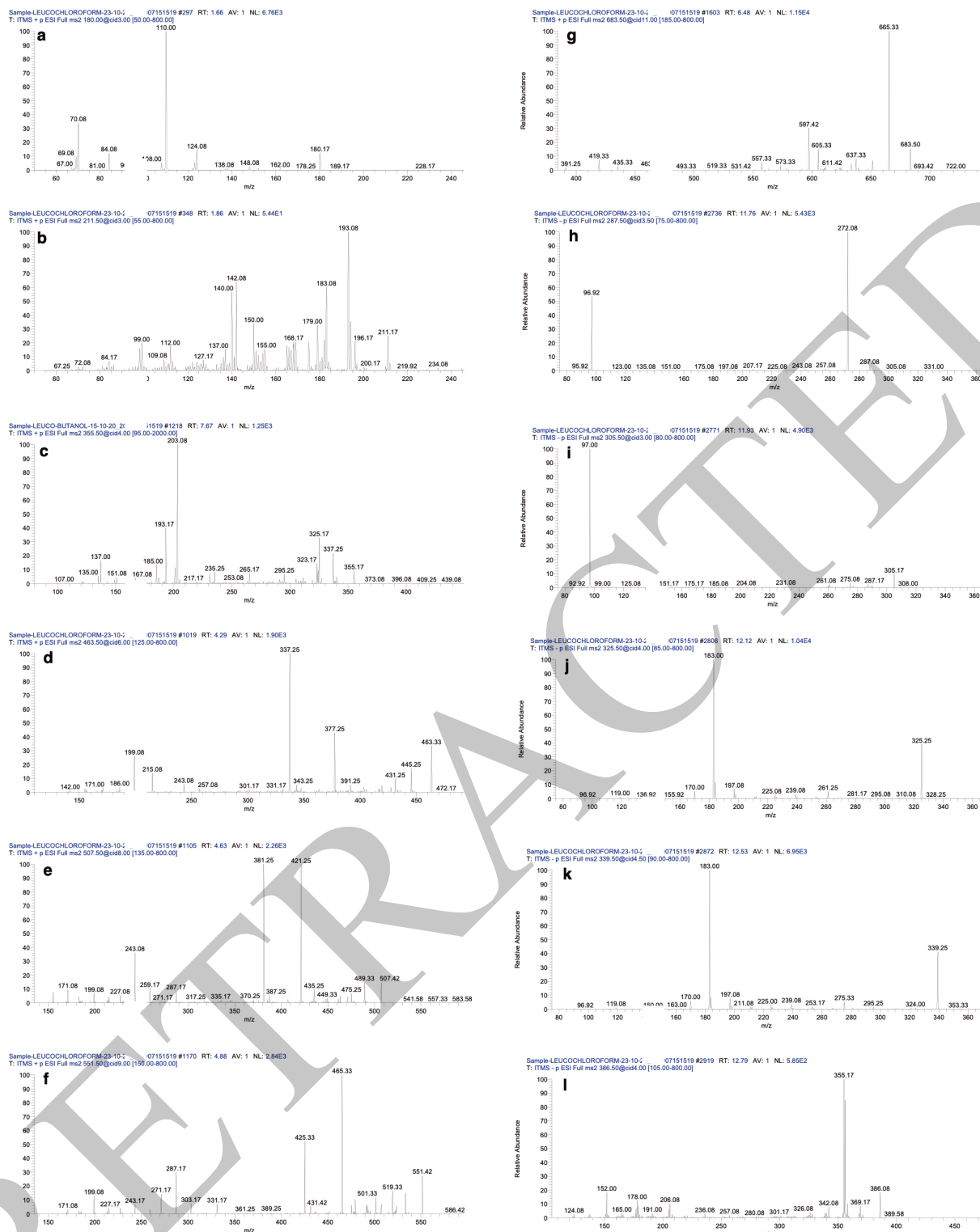


Fig. 2. The ms^2 ionograms a-l of theobromine. (a) propylgallate; (b) asarinin; (c) quercetin-3-beta-glucoside; (d) myricetin-3-acetylramnoside; (e) isoquercitrin-6'-O-malonate; (f) diosmetin-7-O-glucuronide-3'-O-pentose; (g) pinoresinol diglucoside; (h) eriodictoyl; (i) epigallocatechin; (j) methyl gallate derivative; (k) eudesmin; (l) respectively.

2.5 Measuring Antioxidant Activity

Antioxidant activity was measured using five different methods. Total antioxidant activity (TAA) was determined

using the phosphomolybdenum method [15] and the results were expressed as mg ascorbic acid $Eq \cdot g^{-1}$ of dried extract. Free radical scavenging activities of MELE, HELE, CHLE, and BULE were estimated colorimetrically using

Enzyme inhibition potential of *L. frutescens* leaf extracts

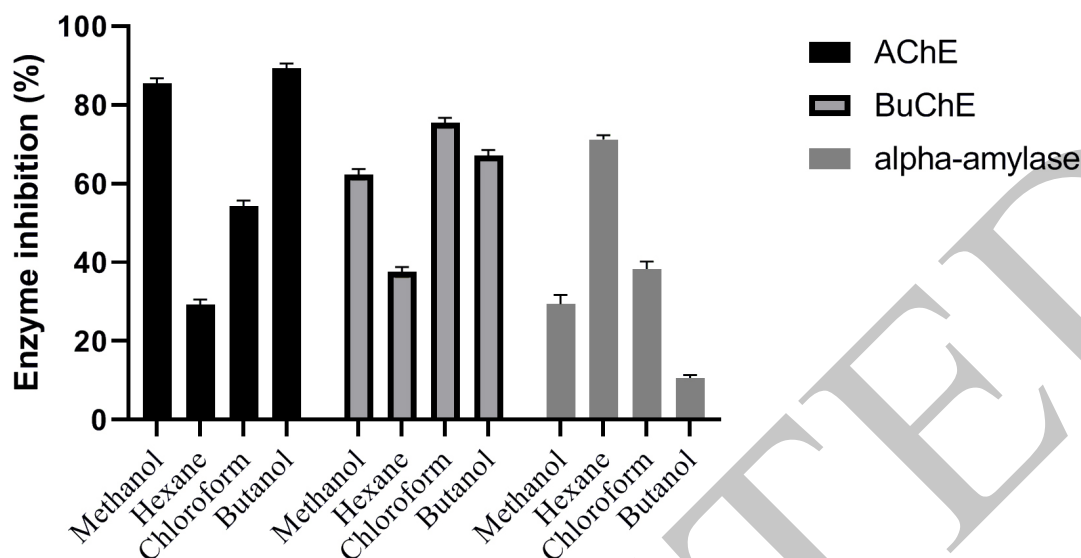


Fig. 3. Inhibition of enzyme activity by methanolic leaf extract (MELE), HELE, CHLE, and BULE of *L. frutescens* leaves. Extracts were prepared with the solvents indicated below the horizontal axis and examined for their ability to inhibit human acetylcholinesterase (acetylcholinesterase (AChE), solid black bars), human butyrylcholinesterase (butyrylcholinesterase (BuChE), gray bars with borders), and human salivary amylase (alpha-amylase, gray bars with no borders). A significant difference ($p < 0.05$) was observed between polar and non-polar solvent fractions for their enzyme inhibition assay.

2,2-diphenyl-1-picrylhydrazyl (DPPH) as an indicator dye [16]. Similarly, free radical scavenging activities were also determined colorimetrically and expressed in the Trolox Equivalent Antioxidant Capacity (TEAC) assay to measure 2'-azinobis-3-(3-ethylbenzothiazoline-6-sulfonic acid) (ABTS) radical bleaching [17]. The metal-reducing potential was also measured by the cupric-reducing antioxidant capacity (CUPRAC) method, which measured the reduction of Cu^{2+} to Cu^{1+} using neocuproine indicator dye [17] and by the ferric-reducing ability of plasma (FRAP) method, which measured the reduction of the ferric tripyridyltriazine (Fe^{3+} -TPTZ) complex [16]. The DPPH, TEAC, CUPRAC, and FRAP antioxidant capacity measurements were expressed as mg Trolox $\text{Eq} \cdot \text{g}^{-1}$ of dried extract.

2.6 Acetylcholinesterase and Butyrylcholinesterase Enzyme Inhibition Activity

Acetylcholinesterase and butyrylcholinesterase enzyme inhibition assay was performed according to a modified version of the Ellman method [5]. The sample solution of the MELE, HELE, CFLE, and BULE was diluted to prepare solutions of different concentrations, including 150, 15.0, 1.5, 0.15, and 0.05 $\mu\text{g} \cdot \text{mL}^{-1}$. Similarly, the eserine solution (1 mg/mL) was serially diluted to produce different calibrators (1000–10 $\text{ng} \cdot \text{mL}^{-1}$). A total of 10.0 μL was added to the respective well of the microplate for

each sample dilution or calibrator, followed by the addition of 30 μL of enzyme solution (0.25 U/mL), and incubated for 30 min at room temperature. Residual enzyme activity was measured by the addition of 10 μL substrate 0.24 mM acetylthiocholine iodide (ATCI) for a period of 20 minutes. Next, 10 μL of indicator (0.2 mM 5,5-dithiobis-2-nitrobenzoic acid (DTNB) in a 0.04 M sodium phosphate buffer at pH 7.5) was added to stop the reaction mixture. After incubating for 5 minutes at room temperature, the absorbance was recorded at 412 nm. The following formula was used for the enzyme inhibition assay:

$$\text{Inhibition (\%)} = \left[1 - \left(\frac{A_{\text{sample}}}{A_{\text{Control}}} \right) \times 100 \right]$$

where A_{sample} is the absorbance of the sample and A_{control} is the absorbance of the solution without the sample.

2.7 Alpha-Amylase Enzyme Inhibition Assay

The ability of the leaf extract samples to inhibit alpha-amylase from human saliva (A1031, type XIII-A) was determined using the 96-microplate spectrophotometric method by Magaji *et al.* [17]. Acarbose was used as a positive control. The percent inhibition was determined using the following formula:

$$\text{Inhibition (\%)} = \left[1 - \left(\frac{A_{\text{sample}}}{A_{\text{Control}}} \right) \times 100 \right]$$

where A_{sample} is the absorbance of the sample and A_{control} is the absorbance of the solution without the sample.

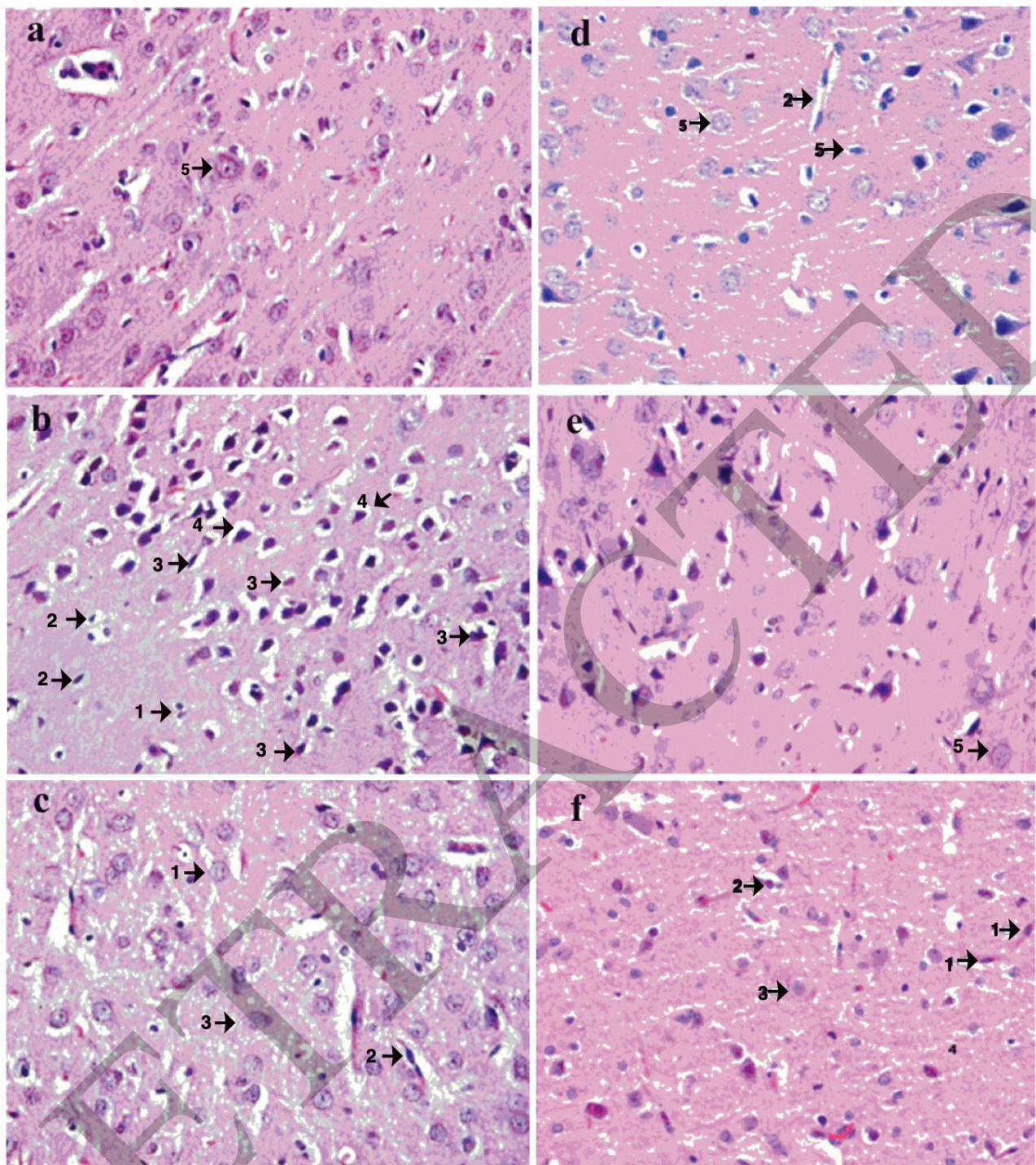


Fig. 4. Effects of BULE *L. frutescens* leaf extract on histopathology in representative photomicrographs of postmortem brain sections of rats administered aluminum chloride-induced (50 mg/kg/day) for 30 days. Photomicrographs are from the following treatment groups: (a) normal control receiving no aluminum chloride; (b) negative control receiving aluminum chloride but no BULE; (c) aluminum chloride-treated rats orally receiving BULE daily at 100 mg/kg/day; (d) aluminum chloride-treated rats orally receiving BULE daily at 200 mg/kg/day; (e) aluminum chloride-treated rats orally receiving BULE daily at 400 mg/kg/day; (f) positive control aluminum chloride treated rats orally receiving rivastigmine daily at 0.4 mg/kg/day. Arrow 1 shows degeneration of glial cells; arrow 2 shows degeneration of pyramidal cells; arrow 3 shows vacuolation of glial cells; arrow 4 shows vacuolation of pyramidal cells; arrow 5 shows normal large vesicular nuclei. The magnification is 40 \times (objective lense SP40/0.65 160mm).

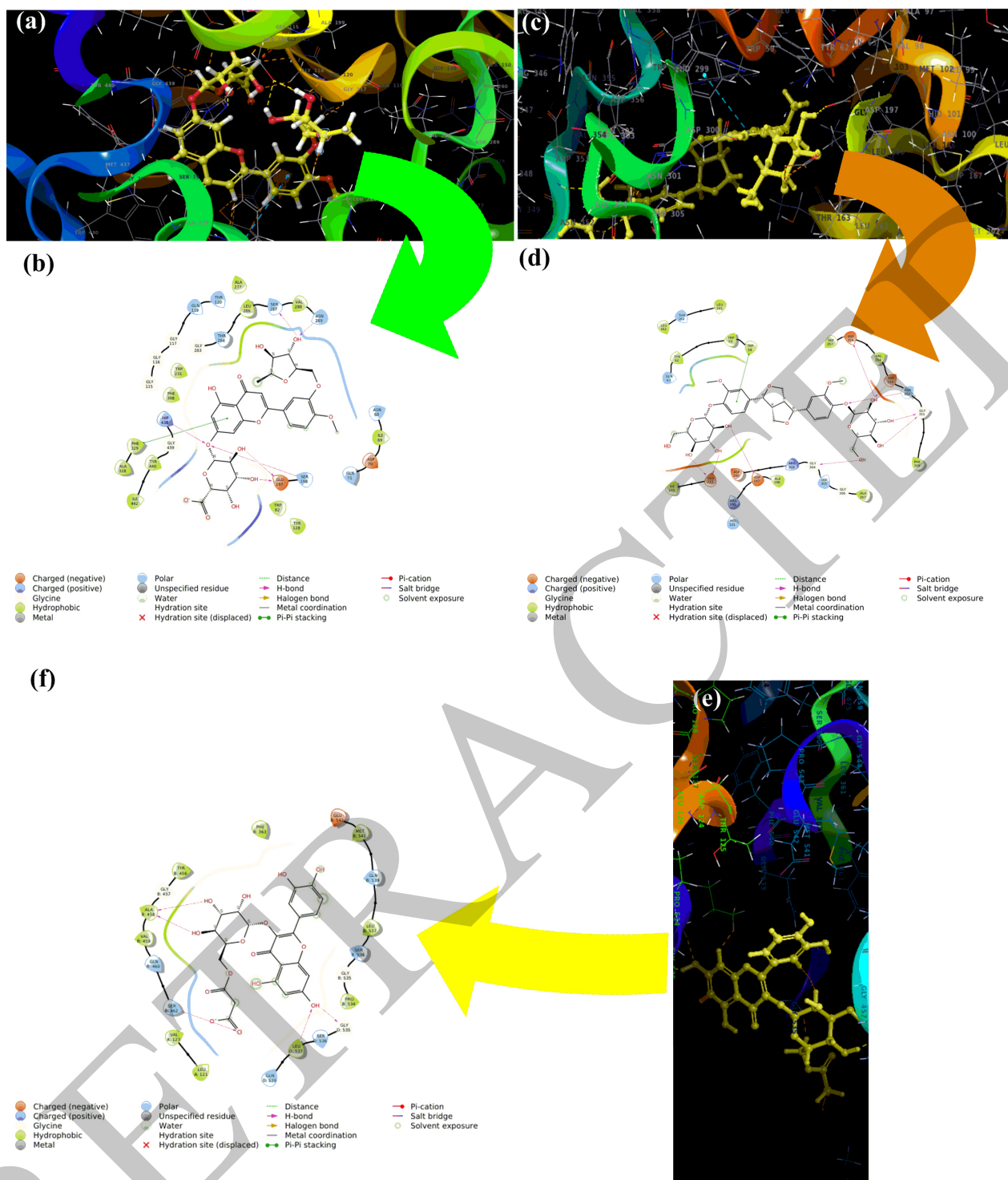


Fig. 5. Molecular modeling of the three *L. frutescens* leaf extract components that bound with the highest affinity to the active sites of the three enzymes clinically linked to neurodegenerative diseases. Diosmetin-7-O-glucuronide-3'-O-pentose docked into the active site of human butyrylcholinesterase (Protein Data Bank code: 4BBZ) and is shown by (a) Three-dimensional and (b) Two-dimensional molecular docking diagrams. Pinoresinol diglucoside docked into the active site of the human salivary amylase (Protein Data Bank Code: 1HNY) and is shown by (c) Three-dimensional and (d) Two-dimensional molecular docking diagrams. (e) Three-dimensional molecular docking diagrams of isoquercetin-6'-O-malonate (Protein Data Bank Code: HM0E) docked into the active site of the human acetylcholinesterase are shown in (e) Three-dimensional and (f) Two-dimensional molecular docking diagrams, respectively.

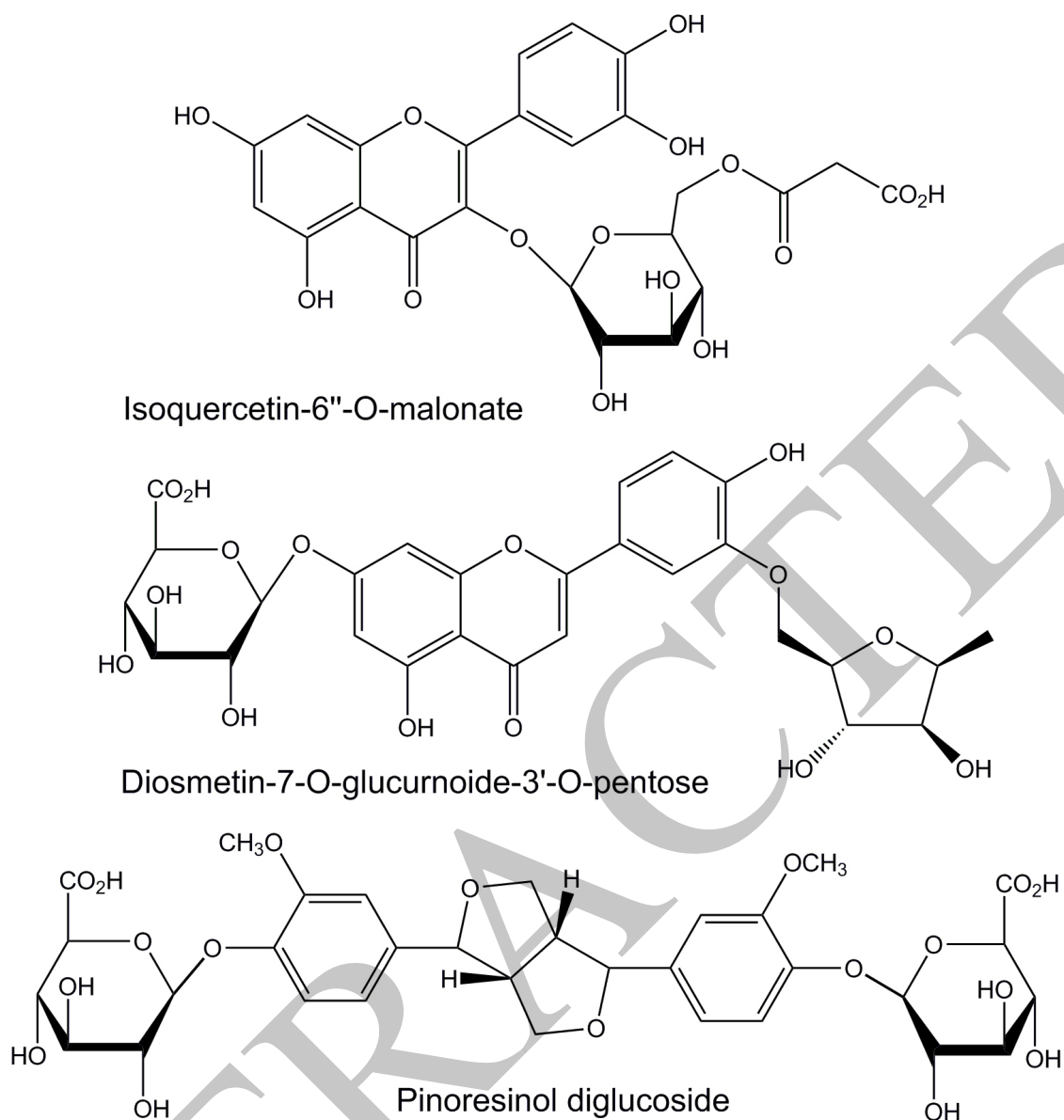


Fig. 6. Structures of *L. frutescens* leaf extract components that bind with the greatest affinity to the active sites of human butyrylcholinesterase (isoquercetin-6'-O-malonate), human acetylcholinesterase (diosmetin-7-O-glucuronide-3'-O-pentose), and human salivary α -amylase (pinoresinol diglucoside).

Calculation of IC_{50}

IC_{50} values of each sample and acarbose were calculated in Microsoft Excel 365 using the linear regression equation.

2.8 Liquid Chromatography–Mass Spectrometric analysis of BULE

The butanol fraction of hydroalcoholic leaf extract (BULE) was investigated using reverse-phase liquid chromatography with mass spectral analysis (LC–MS/MS) in an LTQ XL Linear Ion Trap Mass Spectrophotometer (Thermo Scientific, Waltham, MA, USA), equipped with an electrospray ionization (ESI) source to qualitatively analyze secondary metabolite modalities. The BULE was dissolved in

methanol, filtered through 0.22 μ m, and injected into a direct syringe pump at a flow rate of 8 μ L·min⁻¹. Both positive and negative total ion full scan modes were applied at m/z 50–2000. The source and capillary voltages were fixed at 4.8 kV and 23 V, respectively. The capillary temperature and sheath gas flow (N₂) were kept at 350 °C and 30 arbitrary units, respectively, in both scanning modes. The selected analyte was fragmented at positive and negative ion modes by employing collision-induced dissociation (CID) energy of 35 (percentage of 5 V).

2.9 In Silico Molecular Docking

In silico molecular docking of 11 selected molecules tentatively identified by LC–MS/MS analysis of BULE

Table 1. Estimation of total phenolic content and total flavonoid content in hydroalcoholic leaf extract (MELE) and its fractions *n*-hexane fraction of hydroalcoholic leaf extract (HELE), chloroform fraction of the hydroalcoholic leaf extract (CHLE), and *n*-butanol fraction of the hydroalcoholic leaf extract (BULE) of *L. frutescens* leaves by regression analysis.

Description	Total phenolic content (mg GA·Eq·gm ⁻¹ DE ± S.D)	Total flavonoid content (mg Qu·Eq·gm ⁻¹ DE ± S.D)
MELE	148.243 ± 1.46 ^b	210.164 ± 3.034 ^c
HELE	3.533 ± 0.111 ^d	113.645 ± 2.195 ^d
CHLE	80.232 ± 0.335 ^c	293.343 ± 3.756 ^a
BULE	223.075 ± 1.422 ^a	230.435 ± 1.575 ^b

^{abcd}: means with different lowercase letters in the same column are significantly different by ANOVA ($p < 0.05$).

was performed by using Maestro | Schrödinger Version 12.1.013 MM shares version 4.7.013, released 2019-3, for platform Linux-x86-64 Schrodinger software (Schrödinger LLC, New York, NY, USA). The ligands were docked into the enzymatically active sites of the following crystal structures of proteins imported from the Protein Data Bank (PDB) [18]: human acetylcholinesterase (PDB code: 4M0E), human butyrylcholinesterase (PDB code: 4BBZ), and human salivary alpha-amylase (PDB code: 1NHY). The steps included protein preparation, ligand preparation, receptor grid generation, and ligand-receptor docking. The water molecules and co-crystallized ligands were removed during the protein preparation process. The partial atomic charges were assigned according to the optimized potentials for the liquid simulation (OPLS3) force field. Grid generation was performed by selecting active binding residues for each protein with the binding box set to 30°Å. Ligand preparation was performed by importing ligand molecules that were formally generated using Chem Draw 15.0.0 (Shelton, CT, USA). The docking glide was used for molecular docking by importing the macromolecular grid file and ligand prep file. The binding score and energy were determined by selecting project. The hydrogen- π , π - π , and alkyl- π interactions between ligand and amino acids were studied, and molecular docking scores and energy values (kcal/mol) were calculated and tabulated.

2.10 In Vivo Neuroprotective Evaluation of BULE in Rats

The neuroprotective effects of BULE were assessed *in vivo* by performing a study using the animal model previously described in the literature [19].

2.10.1 Animals

A total of 30 female albino rats, aged 8–10 weeks, were procured from the animal house of the Department of Pharmacology, Islamia University of Bahawalpur, Pakistan. These animals were maintained in a specific pathogen-free environment with a controlled temperature of 25 ± 1 °C and humidity of $55 \pm 2\%$ in a 12-hour alternating light and dark cycle, and fed *ad libitum* until they gained 200–230 g in weight. This study was approved by

the Research and Ethics Committee of the Faculty of Pharmacy, Islamia University of Bahawalpur. Procedures were performed in accordance with the regulations and ethical considerations of international laws and Islamic perspectives [18].

2.10.2 Experimental Design

The animals were divided into five groups “A, B, C, D, E, and F”. Group A served as the normal control. AD was induced in groups B, C, D, E, and F by orally administering aluminum chloride (100 mg/kg/day) for 42 days. Group B served as the negative control (AD induced with no treatment). Groups C, D, and E (AD induced with treatment) were orally administered an aqueous suspension of BULE at doses of 100 mg/kg/day, 200 mg/kg/day, and 400 mg/kg/day, respectively. Group F was orally administered rivastigmine (0.3 mg/kg/day) and served as the positive control. The treatment was performed for a month after the development of AD in all the groups except A (normal control group). The induction of AD was assessed using the Morris water test [19].

2.10.3 Sample Collection

The control and treated rats were sacrificed by cervical dislocation, and their brains were secured and the hippocampus quickly dissected, which was homogenized in 10% w/v ice-cold mixture of 50 mM Tris buffer (Sigma-Aldrich, St. Louis, MO, USA) pH 7.4 and 300 mM sucrose solution using a Potter–Elvehjem homogenizer. The homogenate was centrifuged at 3000 rpm for 10 minutes, and the supernatant was frozen at -80 °C until it was analyzed for acetylcholinesterase levels and butyrylcholinesterase activities.

2.11 Statistical Analysis of Data

Each experiment was performed in triplicate, and values were expressed as the mean \pm standard deviation. Quantitative data were subjected to a one-way ANOVA using the data analysis tool in Microsoft Excel 2019 version 16.0, Microsoft, Redmond, WA, USA to determine significant differences ($p < 0.05$). The linear regression equation

Table 2. Phenolic compounds identified in the chloroform extract of *L. frutescens* leaves using reverse phase liquid chromatography with mass spectrometry.

#	Retention time	ESI mode	Adduct (m/z)	Tentative identification	Class/subclass	Molecular formula	Observed mass	MS ² fragments and reference
1	1.66	Positive mode of ionization	[M+H] ⁺	Theobromine	Alkaloid	C ₁₂ H ₁₀ ClN ₃ S	180.25	138, 110 [20,21]
2	1.86		[M+H] ⁺	Propylgallate	Galloyl ester	C ₁₀ H ₁₂ O ₅	211.50	196, 168, 140 [22]
3	3.67		[M+H] ⁺	Asarinin	Lignan	C ₂₀ H ₁₈ O ₆	355.50	337, 325, 135 [23]
4	4.29		[M+H] ⁺	Quercetin-3-beta-glucoside	Flavonoid glycoside	C ₂₁ H ₂₀ O ₁₂	463.33	337, 301, 215 [20]
5	4.63		[M+H] ⁺	Myricetin 3-acetylramnoside		C ₂₁ H ₂₀ O ₁₂	507.42	421, 381, 317, 287 [24]
6	4.88		[M+H] ⁺	Isoquercitrin 6'-O-malonate	Flavonoid derivative	C ₂₄ H ₂₂ O ₁₅	551.42	465, 303 [25]
7	5.49		[M+H] ⁺	Diosmetin-7-O-glucuronide-3'-O-pentose	Flavonoid glycoside	C ₂₇ H ₂₈ O ₁₇	607.33	547, 531, 487, 473, 461 [26]
8	6.83		[M+H] ⁺	Pinoresinol diglucoside	Lignan glycoside	C ₃₂ H ₄₂ O ₁₆	683.50	665, 519 [27]
9	11.76	Negative mode of ionization	[M-H] ⁻	Eridictyol	Flavonoid	C ₁₅ H ₁₂ O ₆	287.08	151, 135, 96 [28]
10	11.93		[M-H] ⁻	Epigallocatechin		C ₂₂ H ₁₈ O ₁₁	305.17	275, 261, 125, 97, 54 [29]
11	12.12		[M-H-142] ⁻	Methyl gallate derivative	Galloyl ester	[C ₈ H ₈ O ₅]-R	325.25	18, 169 [30]
12	12.53		[M-H-154] ⁻			[C ₈ H ₈ O ₅]-R	339.25	183, 170 [30]
13	12.79		[M] ⁻	Eudesmin	Lignan	C ₂₂ H ₂₆ O ₆	386.08	369, 355, 342, 206, 165 [31]

in the Microsoft 2019 data analysis tool was used to calculate radical scavenging and antioxidant potentials and half-maximal enzyme inhibitory concentration (IC₅₀) values.

3. Results and Discussion

3.1 Phenolic and Flavonoid Contents of *L. frutescens* Leaf Extracts

Polyphenols are plant components that include chlorogenic acids, tannins, hydrolyzable tannins, flavonoids, and lignans, which are found mostly as glycosides in undisturbed tissues but may be released as biologically active aglycones by glycosidase during predation or extraction. Polyphenols are potentially useful as nutraceuticals and perform a variety of pharmacological effects on the body after consumption, based on their antibacterial, antiviral, antiparasitic, antidiabetic, anticancer, and antioxidant properties [20].

Phytochemical analysis of *L. frutescens* hydroalcoholic leaf extract and its fractions confirmed the presence of alkaloids, phenols, flavonoids, saponins, and glycosides. BULE exhibited the highest total phenolic content, while HELE exhibited the lowest (Table 1). The TPC and TFC contents of this study were compared to a previous study

conducted on the aerial parts of *L. frutescens*, which revealed a significant difference in the polar fractions of TPC and TFC, where the highest TPC was determined as 189.369 ± 1.393 mg GA·Eq·gm⁻¹ DE \pm S.D by BULE and TFC was determined as 232.458 ± 1.589 mg Qu·Eq·gm⁻¹ DE \pm S.D by CHLE [13].

The LC-MS² analysis tentatively identified 14 compounds belonging to the alkaloid, flavonoid, flavonoid glycoside, lignan, and lignan glycoside groups. These tentatively identified compounds were theobromine, propyl gallate, quercetin-3-O-glucoside, myricetin 3-acetylramnoside, isoquercitrin-6'-O-malonate, diosmetin-7-O-glucuronide-3'-O-pentose, pinoresinol diglucoside, asarinin, eridictyol, epigallocatechin, methyl gallate derivative, eudesmin, and aschantin (Table 2, (Ref. [20–31]) and Fig. 2).

3.2 Antioxidant Activity

Excessive accumulation of reactive oxygen species (ROS) is believed to play a role in Alzheimer's disease via the accumulation of beta-amyloid protein in the neuronal tissues [32]. The radical scavenging potentials determined by DPPH and TEAC were as follows: CHLE > MELE >

Table 3. Antioxidant potential of methanolic extract (MELE) and its fractions HELE, CHLE, and BULE.

Description	TAA	DPPH	TEAC	CUPRAC	FRAP
	mg AA·Eq·gm ⁻¹	mg· trolox Eq·gm ⁻¹	mg· trolox Eq·gm ⁻¹	mg· trolox Eq·gm ⁻¹	mg· trolox Eq·gm ⁻¹
	DE ± S.D	DE ± S.D	DE ± S.D	DE ± S.D	DE ± S.D
MELE	152.603 ± 1.506	171.336 ± 3.750	170.866 ± 2.340	356.343 ± 4.860	335.232 ± 2.840
HELE	166.625 ± 2.133	84.247 ± 4.340	70.570 ± 4.440	249.121 ± 4.770	190.232 ± 3.560
CHLE	194.046 ± 1.150	215.235 ± 4.450	220.243 ± 3.660	536.336 ± 5.740	482.434 ± 1.434
BULE	226.236 ± 1.222	160.286 ± 3.335	158.232 ± 3.550	450.236 ± 4.640	350.323 ± 1.164

All values are expressed as mean ± S.D for triplicates; AA·Eq, ascorbic acid equivalent; IC₅₀, 50% inhibitory concentration; S.D, standard deviation; TAA, total antioxidant activity; DPPH, 2,2-diphenyl-1-picrylhydrazyl; TEAC, Trolox equivalent antioxidant capacity; CUPRAC, cupric-reducing capacity; FRAP, ferric-reducing antioxidant potential.

Table 4. Inhibition of human cholinesterase and α-amylase enzymes by solvent extracts of *L. frutescens* leaves.

Test materials	Acetylcholinesterase inhibition		Butyrylcholinesterase inhibition		α-amylase inhibition	
	% inhibition	IC ₅₀	% inhibition	IC ₅₀	% inhibition	IC ₅₀
	(0.5 mg·mL ⁻¹)	(μg·mL ⁻¹)	(0.5 mg·mL ⁻¹)	(μg·mL ⁻¹)	(5 mg·mL ⁻¹)	(mg·mL ⁻¹)
MELE	85.5 ± 1.4	62.9 ± 1.3	62.4 ± 1.3	249.8 ± 1.2	29.4 ± 0.2	10.0 ± 0.8
HELE	29.3 ± 1.3	>500	37.6 ± 1.3	>500	71.2 ± 3.5	2.9 ± 0.3
CHLE	54.3 ± 1.5	428.6 ± 1.2	75.4 ± 1.3	129.7 ± 1.1	38.3 ± 2.6	6.7 ± 0.2
BULE	89.3 ± 1.2	12.1 ± 0.9	67.2 ± 1.3	156.3 ± 1.3	10.9 ± 0.7	>10
Eserine	91.5 ± 1.3	0.7 ± 0.0	ND	2.3 ± 0.1	ND	ND
Acarbose	ND	ND	ND	ND	98.9 ± 0.2	0.1 ± 0.01

Abbreviations: IC₅₀, half maximal inhibitory concentration; ND, not done.

BULE > HELE (Table 3). The total antioxidant activity of CHLE was significantly higher ($p < 0.05$) than HELE. Similarly, CHLE also reported higher scavenging potential by DPPH and TEAC and high metal-reducing potential compared to MELE, CHLE, and HELE.

3.3 Enzyme Inhibition Assays

Acetylcholinesterase (AChE) and butyrylcholinesterase (BChE) were inhibited by sample extracts and the positive controls, eserine and acarbose (Fig. 3 and Table 4). BULE exhibited significant inhibitory activity against AChE, whereas CHLE exhibited the highest inhibitory activity against BChE, which was consistent with them being the best starting sources for bioassay-guided purification of AChE and butyrylcholinesterase (BuChE) inhibitors. Phytochemical analysis and spectroscopic techniques indicated the presence of lignans and alkaloids in the leaves of *L. frutescens*.

Inhibition of glucose production from starch is one of several mechanisms used by effective antidiabetic drugs. By delaying starch digestion, alpha-amylase inhibitor drugs, such as acarbose, slow glucose production, and hence, absorption, resulting in reduced postprandial elevation of blood glucose. Type 3 diabetes mellitus (Type 3 DM) has been proposed to represent a major pathogenic mechanism of AD neurodegeneration. Type 3 DM corresponds to a state of chronic insulin resistance plus insulin deficiency, which is largely confined to the brain, yet, as in the case of non-alcoholic steatohepatitis (NASH), it can

overlap with Type 2 DM. The study by De La Monte *et al.* [33] examined the postmortem brain tissue and found that AD may be associated with insulin signaling. Additionally, other studies linking diabetes with AD have focused on Type 2 diabetes as a cause of insulin resistance, oxidative stress, and cognitive impairment, although the aggregate of these effects still falls short of mimicking AD [34]. The HELE exhibited high alpha-amylase enzyme inhibition (see Table 3); this activity is potentially useful for decreasing blood sugar levels and ultimately decreasing oxidative stress, which is one of the factors involved in AD. The literature review revealed various classes of lignans, including those identified as present in BULE, effectively controlled plasma glucose levels in the diabetes-induced albino rat model [35]. The only alkaloid tentatively identified in BULE was theobromine. Theobromine is also a prescription drug, which is used against bronchoconstriction due to its vasodilating effects. Since recent studies have indicated that high cholesterol levels can contribute to AD development, theobromine was evaluated for its effects on cognitive behavior changes in albino rats fed a lard-enriched diet. Interestingly, it was shown to improve cognitive functions due to the restoration of A1 receptors and beta-amyloid [36].

3.4 Neuroprotective Effect of BULE against Aluminum Chloride-Induced Hippocampus Damage in Rats

The AChE and BuChE *in vitro* enzyme inhibition assay revealed that BULE showed the highest potential

Table 5. Interaction of selected phytochemicals in *n*-butanol extracts of *L. frutescens* leaves with the active sites of human butyrylcholinesterase, human acetylcholinesterase, and human pancreatic alpha-amylase.

Compound	Butyrylcholinesterase		Acetylcholinesterase		Human pancreatic alpha-amylase	
	(PDB code: 4BBZ)		(PDB code: 4M0E)		(PDB code: 1HNY)	
	Binding affinity (kcal/mol)	Interacting amino acid(s) and position number(s)	Binding affinity (kcal/mol)	Interacting amino acid(s) and position number(s)	Binding affinity (kcal/mol)	Interacting amino acid(s) and position number(s)
Asarinin	−7.395	Trp 231, Trp 430	−3.632	Thr 125	−5.365	Trp 59, Gln 63, His 201
Aschantin	−6.691	Ser 198, Trp 82	−4.377	Thr 125, Ala 458,	−4.904	Gln 63, Thr 163, His 305
Diosmetin-7-O-glucuronide-3'-O-pentose	−9.268	Glu 197, Ser 287, Asn 189, Ser 198, His 438, Phe 329	−6.743	Val 122, Ser 462, Gln 461, Val 459, Ala 458, Gln 539, Glu 542	−7.247	Asn 53, Try 58, Trp 59, Asp 197, Arg 195, Glu 233
Epigallocatechin	−8.104	Thr 120, Asp 70, His 438, Glu 197	−5.469	Thr 125, Gly 535	−6.840	Thr 163, Asp 197, Glu 233
Eudesmin	−5.597	Ser 198, Phe 329, His 438		Thr 125, Ala 458	−4.697	Gln 63
Isoquercetin-6'-O-malonate	−10.533	Gly 115, Gly 116, Glu 197, Trp 82, Ala 328, Pro 285	−5.339	Ser 462, Ala 458, Gly 535, Leu 537	−6.855	Gln 63, Trp 59, Trp 58, Asp 356, Asp 300
Myricetin-3-O-acetylramnoside	−9.844	Asn 83, Glu 197, Ser 198, Ser 287, His 438	−5.469	Gln 539, Gly 535, Leu 537, Glu 542	−6.796	Trp 59, Gln 63, Asn 352, Asp 356
Pinoresinol diglucoside	−9.071	Glu 197, Tyr 332, Phe 329, His 438, Ser 287, Asn 289	−6.575	Val, 122, Thr 125, Tyr 456, Glu 542, Gln 460, Pro 534, Ser 462	−7.888	Trp 58, Asp 197, Glu 233, Gly 304, Gly 351, Asn 352
Propyl gallate	−3.526	Ser 198, Gly 116, Glu 197, His 438	−3.911	Gly 535, Gln 539	4.641	Gln 63
Sesamin	−7.955	Trp 231, Trp 430.	−4.233	-	4.681	Gln 63
Eridictoyl	−8.927	Gly 115, Glu 197, Ser 198	−4.733	-	−6.158	Gln 63, Trp 59, Glu 233, Arg 195, Asp 197

against AChE among all tested samples. Therefore, the *in vivo* neuroprotective effect of BULE was investigated in female albino rats where hippocampal damage had previously been induced by oral administration of aluminum chloride at 100 mg/kg/day for 42 days. The neuroprotective effects of BULE were demonstrated in animal groups treated with BULE and the positive control (rivastigmine) by a reduction in the following degenerative changes: decreased cellular population, increased cellular degeneration signs, and hypertrophy due to an enlargement in the mononucleate cells (Fig. 4).

3.5 In Silico Molecular Docking of Selected *L. frutescens* Leaf Extract Components

The effects on the enzymes involved in neurodegeneration, which could be exerted by a series of 11 *L. frutescens* leaf extract components that had been identified by LC-MS/MS, were further characterized using computational

chemistry to dock the molecules into the active sites of human acetylcholinesterase (PDB code: 4M0E), human butyrylcholinesterase (PDB code: 4BBZ), and human salivary alpha-amylase (PDB code: 1HNY). The binding affinity, binding energy, and amino acids interacting with the enzyme active sites were determined for each of the 11 components identified in BULE and are presented in Table 5. The interactions of the three *L. frutescens* leaf extract components with the highest binding affinities to the active sites of the three enzymes were modeled and the interactions are shown in Fig. 5. The binding of the *L. frutescens* leaf extract components to the active sites predominantly resulted from one or both of the two types of interactions: hydrogen bonding and π - π stacking. Isoquercetin-6'-O-malonate bound to butyrylcholinesterase with the greatest affinity at −10.533 kcal/mol (Table 4) and was shown to interact with the following amino acids at the indicated polypeptide chain number: Trp82, Gly115, Gly116, Glu197, Pro285, and Ala328,

using hydrogen binding and π - π stacking (Fig. 5). The *L. frutescens* leaf extract component that bound to acetylcholinesterase with the greatest affinity was diosmetin-7-O-glucuronide-3'-O-pentose at -6.743 kcal/mol and it was shown to interact with Val122, Ser462, Gln461, Val459, Ala458, Gln539, and Glu542 residues through hydrogen bonding. The *L. frutescens* leaf extract component with the highest binding affinity to the active site of the human salivary alpha-amylase was pinorelinol diglucoside, which had a binding affinity of -7.888 kcal/mol and resulted from interactions through hydrogen bonding to amino acid residues Trp58, Asp197, Glu233, Gly304, Gly351, and Asn352.

Herbal medications are generally complex mixtures of substances that usually have different mechanisms of action. Thus, they have the potential to use multiple mechanisms simultaneously to treat disease conditions that respond to combination therapy. In the case of attempting to use *L. frutescens* leaf extracts for neuroprotection, the three identified component phytochemicals that bound with the highest affinity to the active sites of the three mediator enzymes had very limited structural similarity (Fig. 6). These three components all have aromatic, polyphenolic core structures with peripheral glycoside moieties. The two that bind to acetylcholinesterase are flavonoid glycosides with saccharide-like free hydroxyl groups in the 3-region of the flavonoid core.

4. Conclusions

Polar solvent extracts of *L. frutescens* leaves containing polyphenols with significant antioxidant activities as measured by five different methods. BULE, the *n*-butanol extract, which exhibited high biological activity levels, contained many phytochemicals, 14 of which could be identified by LC-MS² and were shown to be predominantly flavonoids and lignans. BULE was shown to contain components that inhibit human enzymes that are clinically linked to neurodegenerative diseases, including butyrylcholinesterase, acetylcholinesterase, and salivary amylase. Further evaluation of 11 known components in BULE using computational chemistry showed that, among those components, isoquercetin-6'-O-malonate bound with the highest affinity to the active site of human butyrylcholinesterase, diosmetin-7-O-glucuronide-3'-O-pentose bound with the highest affinity to the active site of human acetylcholinesterase, and pinorelinol diglucoside bound with the highest affinity to the active site of human salivary alpha-amylase. BULE also provided neuroprotective effects against aluminum chloride-induced hippocampus damage in albino rats. These results indicate the need for further studies on *L. frutescens* leaf extracts to identify possible neuroprotective agents using bioassay-guided fractionation and other research methodologies.

Availability of Data and Materials

Datasets used and/or analyzed for this study are available from the corresponding author upon appropriate request.

Author Contributions

Conceptualization: IA, EKA, and WTS; methodology: IA, SA, HR, and NS; validation: IA and NS; formal analysis: IA, NS, and MN; investigation: IA, BA, and WTS; data curation: IA, EKA, BA and ES-S; writing-original draft preparation: IA, EKA and ES-S; writing-review and editing: IA, EKA, and ES-S. All authors contributed to editorial changes in the manuscript. All authors read and approved the final manuscript. All authors have participated sufficiently in the work to take public responsibility for appropriate portions of the content and agreed to be accountable for all aspects of the work in ensuring that questions related to its accuracy or integrity.

Ethics Approval and Consent to Participate

This study was approved by the Advanced Studies & Research Board of the Islamia University of Bahawalpur via letter No. 673/AS&RB dated December 16, 2019. This study was approved by the Research and Ethics Committee of the Faculty of Pharmacy, Islamia University of Bahawalpur Procedures.

Acknowledgment

Not applicable.

Funding

This research received no external funding.

Conflict of Interest

The authors declare no conflict of interest. EKA had served as one of the Guest editors of this journal. We declare that EKA had no involvement in the peer review of this article and has no access to information regarding its peer review. Full responsibility for the editorial process for this article was delegated to Luigi De Masi.

References

- [1] Calsolaro V, Bottari M, Coppini G, Lemmi B, Monzani F. Endocrine dysfunction and cognitive impairment. *Minerva Endocrinology*. 2021; 46: 335–349.
- [2] Wu Y, Wu H, Zeng J, Pluimer B, Dong S, Xie X, *et al.* Mild traumatic brain injury induces microvascular injury and accelerates Alzheimer-like pathogenesis in mice. *Acta Neuropathologica Communications*. 2021; 9: 74.
- [3] Cummings JL, Cole G. Alzheimer disease. *Journal of the American Medical Association*. 2002; 287: 2335–2338.
- [4] Mayeux R, Stern Y. Epidemiology of Alzheimer disease. *Cold Spring Harbor Perspectives in Medicine*. 2012; 2: a006239.
- [5] Balkrishna A, Pokhrel S, Tomer M, Verma S, Kumar A, Nain P, *et al.* Anti-Acetylcholinesterase Activities of Mono-Herbal Extracts and Exhibited Synergistic Effects of the Phytocon-

- stituents: A Biochemical and Computational Study. *Molecules*. 2019; 24: 4175.
- [6] Yan, W. Acetylcholinesterase inhibition effect of flavonoids from *Flemingia philippinensis*. *Science and Technology of Food Industry*. 2021; 42: 118.
 - [7] Dos Santos Maia M, Rodrigues GCS, de Sousa NF, Scotti MT, Scotti L, Mendonça-Junior FJB. Identification of New Targets and the Virtual Screening of Lignans against Alzheimer's Disease. *Oxidative Medicine and Cellular Longevity*. 2020; 2020: 3098673.
 - [8] Zhou L, Han FY, Lu LW, Yao GD, Zhang YY, Wang XB, *et al.* Isolation of enantiomeric furofuranones and furofurans from *Rubus idaeus* L. with neuroprotective activities. *Phytochemistry*. 2019; 164: 122–129.
 - [9] Han Y, Kim SJ. Memory enhancing actions of *Asiasari radix* extracts via activation of insulin receptor and extracellular signal regulated kinase (ERK) I/II in rat hippocampus. *Brain Research*. 2003; 974: 193–201.
 - [10] Sims-Robinson C, Kim B, Rosko A, Feldman EL. How does diabetes accelerate Alzheimer disease pathology? *Nature Reviews. Neurology*. 2010; 6: 551–559.
 - [11] Mettupalayam Kaliyannan Sundaramoorthy P, Kilavan Packiam K. *In vitro* enzyme inhibitory and cytotoxic studies with *Evolvulus alsinoides* (Linn.) Linn. Leaf extract: a plant from Ayurveda recognized as *Dasapushpam* for the management of Alzheimer's disease and diabetes mellitus. *BMC Complementary Medicine and Therapies*. 2020; 20: 129.
 - [12] Nair SS, Kavrekar V, Mishra A. *In vitro* studies on alpha amylase and alpha glucosidase inhibitory activities of selected plant extracts. *European Journal of Experimental Biology*. 2013; 3: 128–132.
 - [13] Ahmad I, Ahmed S, Küpeli Akkol E, Rao H, Shahzad MN, Shaukat U, *et al.* GC-MS profiling, phytochemical and biological investigation of aerial parts of *Leucophyllum frutescens* (Berl.) IM Johnston (Cenizo). *South African Journal of Botany*. 2022; 148: 200–209.
 - [14] Evans WC. Trease and Evans' Pharmacognosy E-book. Elsevier Health Sciences: United Kingdom. 2009.
 - [15] Govindarajan R, Rastogi S, Vijayakumar M, Shirwaikar A, Rawat AKS, Mehrotra S, *et al.* Studies on the antioxidant activities of *Desmodium gangeticum*. *Biological & Pharmaceutical Bulletin*. 2003; 26: 1424–1427.
 - [16] Grochowski DM, Uysal S, Zengin G, Tomczyk M. *In vitro* antioxidant and enzyme inhibitory properties of *Rubus caesius* L. *International Journal of Environmental Health Research*. 2019; 29: 237–245.
 - [17] Magaji UF, Sacan O, Yanardag R. Alpha amylase, alpha glucosidase and glycation inhibitory activity of *Moringa oleifera* extracts. *South African Journal of Botany*. 2020; 128: 225–230.
 - [18] Naderi MM, Sarvari A, Milanifar A, Boroujeni SB, Akhondi MM. Regulations and ethical considerations in animal experiments: international laws and Islamic perspectives. *Avicenna Journal of Medical Biotechnology*. 2012; 4: 114–120.
 - [19] Kasbe P, Jangra A, Lahkar M. Mangiferin ameliorates aluminium chloride-induced cognitive dysfunction via alleviation of hippocampal oxido-nitrosative stress, proinflammatory cytokines and acetylcholinesterase level. *Journal of Trace Elements in Medicine and Biology: Organ of the Society for Minerals and Trace Elements (GMS)*. 2015; 31: 107–112.
 - [20] Mocan A, Schafberg M, Crişan G, Rohn S. Determination of lignans and phenolic components of *Schisandra chinensis* (Turcz.) Baill. using HPLC-ESI-ToF-MS and HPLC-online TEAC: Contribution of individual components to overall antioxidant activity and comparison with traditional antioxidant assays. *Journal of Functional Foods*. 2016; 24: 579–594.
 - [21] Mendes VM, Coelho M, Tomé AR, Cunha RA, Manadas B. Validation of an LC-MS/MS Method for the Quantification of Caffeine and Theobromine Using Non-Matched Matrix Calibration Curve. *Molecules*. 2019; 24: 2863.
 - [22] Riaz M, Rasool N, Iqbal M, Tawab A, Habib FE, Khan A, *et al.* Liquid chromatography-electrospray ionization-tandem mass spectrometry (LC-ESI-MS/MS) analysis of *Russelia equisetiformis* extract. *Bulgarian Chemical Communications*. 2017; 49: 354–359.
 - [23] Kumar V, Kumar S, Singh B, Kumar N. Quantitative and structural analysis of amides and lignans in *Zanthoxylum armatum* by UPLC-DAD-ESI-QTOF-MS/MS. *Journal of Pharmaceutical and Biomedical Analysis*. 2014; 94: 23–29.
 - [24] Bravo MN, Silva S, Coelho AV, Vilas Boas L, Bronze MR. Analysis of phenolic compounds in Muscatel wines produced in Portugal. *Analytica Chimica Acta*. 2006; 563: 84–92.
 - [25] Lin LZ, He XG, Lindenmaier M, Yang J, Cleary M, Qiu SX, *et al.* LC-ESI-MS study of the flavonoid glycoside malonates of red clover (*Trifolium pratense*). *Journal of Agricultural and Food Chemistry*. 2000; 48: 354–365.
 - [26] Al-Yousef HM, Hassan WHB, Abdelaziz S, Amina M, Adel R, El-Sayed MA. UPLC-ESI-MS/MS profile and antioxidant, cytotoxic, antidiabetic, and antiobesity activities of the aqueous extracts of three different *Hibiscus* species. *Journal of Chemistry*. 2020; 2020: 6749176.
 - [27] Kwon D, Kim GD, Kang W, Park J-E, Kim SH, Choe E, *et al.* Pinorensinol diglucoside is screened as a putative α -glucosidase inhibiting compound in *Actinidia arguta* leaves. *Journal of the Korean Society for Applied Biological Chemistry*. 2014; 57: 473–479.
 - [28] Lin LZ, Mukhopadhyay S, Robbins RJ, Harnly JM. Identification and quantification of flavonoids of Mexican oregano (*Lippia graveolens*) by LC-DAD-ESI/MS analysis. *Journal of Food Composition and Analysis: an Official Publication of the United Nations University, International Network of Food Data Systems*. 2007; 20: 361–369.
 - [29] Tang J, Dunshea FR, Suleria HAR. LC-ESI-QTOF/MS Characterization of Phenolic Compounds from Medicinal Plants (Hops and Juniper Berries) and Their Antioxidant Activity. *Foods*. 2019; 9: 7.
 - [30] Flamini R. Recent applications of mass spectrometry in the study of grape and wine polyphenols. *International Scholarly Research Notices*. 2013; 2013: 45.
 - [31] Schmidt TJ, Hemmati S, Fuss E, Alfermann AW. A combined HPLC-UV and HPLC-MS method for the identification of lignans and its application to the lignans of *Linum usitatissimum* L. and *L. bienne* Mill. *Phytochemical Analysis: PCA*. 2006; 17: 299–311.
 - [32] Bai M, Yao G-D, Liu S-F, Wang D, Liu Q-B, Huang X-X, *et al.* Lignans from a wild vegetable (*Patrinia villosa*) able to combat Alzheimer's disease. *Journal of Functional Foods*. 2017; 28: 106–113.
 - [33] de la Monte SM, Wands JR. Alzheimer's disease is type 3 diabetes-evidence reviewed. *Journal of Diabetes Science and Technology*. 2008; 2: 1101–1113.
 - [34] Kroner Z. The relationship between Alzheimer's disease and diabetes: Type 3 diabetes? *Alternative Medicine Review: a Journal of Clinical Therapeutic*. 2009; 14: 373–379.
 - [35] Xu Z, Wang X, Zhou M, Ma L, Deng Y, Zhang H, *et al.* The antidiabetic activity of total lignan from *Fructus Arctii* against alloxan-induced diabetes in mice and rats. *Phytotherapy Research: PTR*. 2008; 22: 97–101.
 - [36] Mendiola-Precoma J, Padilla K, Rodríguez-Cruz A, Berumen LC, Miledi R, García-Alcocer G. Theobromine-Induced Changes in A1 Purinergic Receptor Gene Expression and Distribution in a Rat Brain Alzheimer's Disease Model. *Journal of Alzheimer's Disease: JAD*. 2017; 55: 1273–1283.